Supplementary Information:

I. Synthesis and characterization of mono and bis terpyridine functionalized poly(ethylene oxide)

Mono and bis-terpyridine-functionalized poly(ethylene oxide) were synthesized by reacting hydroxyl-terminated poly(ethylene oxide) with 4'-chloro-2,2':6'2''-terpyridine in the presence of KOH in DMSO at 70°C. The detailed experimental procedure for the synthesis of the bis-terpyridine-functionalized poly(ethylene oxide) is the following: 10 g (1 mmol) of dihydroxy-terminated linear poly(ethylene oxide) and 560 mg (0.01 mol) of KOH were dissolved in 200 mL of dry DMSO. The solution was purged with argon for 30 min. 4'-chloro-2,2':6'2''-terpyridine (1.071 g: 4 mmol) was added to the reaction mixture under continuous stirring. Then, the reaction was stirred for 5 days at 70°C. The accordingly obtained mono and bis-terpyridine functionalized poly(ethylene oxide) were characterized by ^{1}H NMR spectroscopy (Figure S1). Figure S1 shows the characteristic signals at 4.4 ppm (labelled c) and between 7.3 and 8.7 ppm (labelled d, e, f, g and h) corresponding to the CH_2 of the EO unit adjacent to the ester group and to of the protons of the terpyridine group, respectively. The ratio of integrated signals corresponding to the -CH (labelled d) of the terpyridine group and the -CH_2 (labelled a,b) of the EO units confirms the quantitative nucleophilic substitution of hydroxyl-end groups of poly(ethylene oxide) chains.

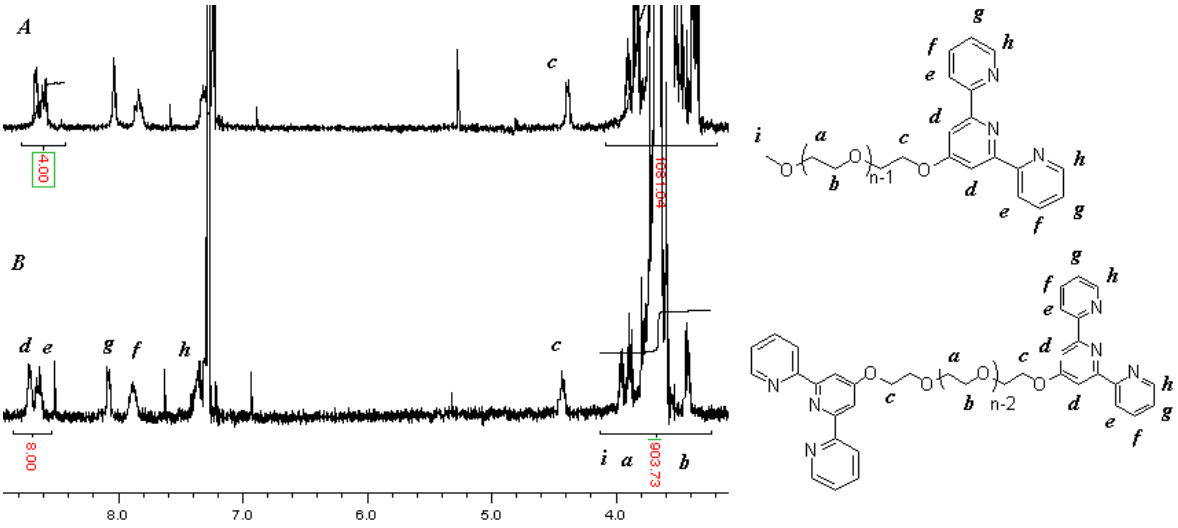

Figure S1. ^{1}H NMR spectra of mono (A) and bis (B) terpyridine-functionalized poly(ethylene oxide) in $CDCl_3$.

II. SAXS measurements

The configuration of terpyridine groups in PEO melt for sample Bi-PEO_0.5eq has been investigated by SAXS measurements, in order to confirm that in the melt, the complexation of chelating terpyridine only results in linearly structured supramolecular polymers.

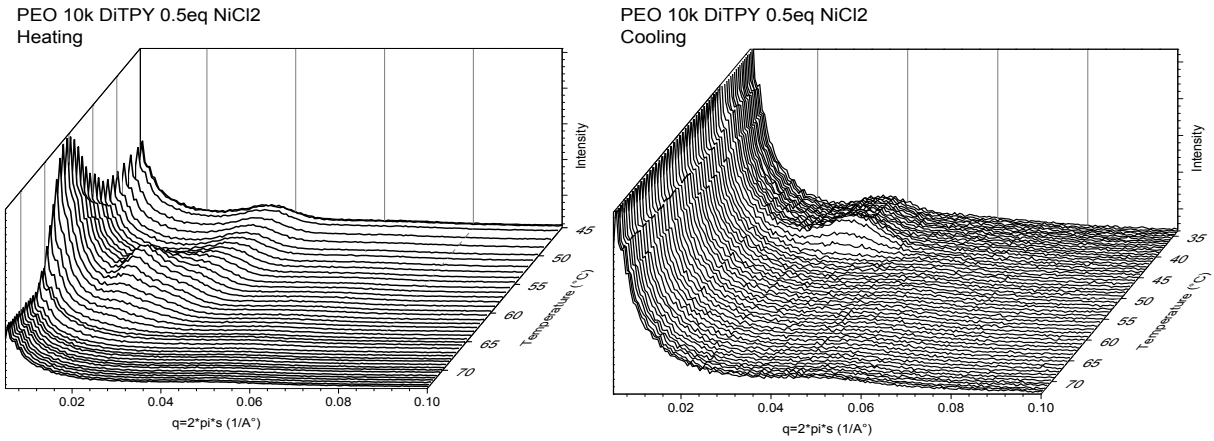

Figure S2: Time resolved SAXS spectra of sample Bi-PEO_0.5eq upon heating (a) and cooling (b). Above melting temperature no long range ordering was observed in the q space spanning from 0.005-0.14 °A^{-1}.

As it is observed in Figure S2.a, upon heating, SAXS data showed four different regions with respect to temperature. First, below the onset of melting (T < 52°C), we observe a constant long range ordering and scattering intensity, which corresponds to constant lamellar thickness and crystalline content. Then, in the second temperature region, which corresponds to the onset of melting up to the melting peak (52°C<T<59°C), we observe an increase in lamellar thickness and overall crystallinity. We shall note that similar lamellar thickness evolution was reported by Cheng et al., who attributed it to the transformation of non-integral folding to integral folding chain crystals.[1,2] Then, in region 3 (59°C<T<65°C), Bragg maxima disappear without much change in lamellar thickness. Finally region 4 corresponds to temperature above the melting temperature. Clearly, in this region, the data do not show any Bragg diffraction maximum and thus, do not reveal any long range ordering neither in heating nor in cooling. Hence we conclude that in this sample, there is no lateral structure due to pi-pi stacking of terpyridine groups in the melt state. This is probably due to the relatively large size of PEO precursors, which dilute the terpyridine groups and separate them apart.

III. Tube based model – Time Marching Algorithm (TMA)

Starting from the MMD of a linear polymer, the TMA model allows us to determine the corresponding relaxation modulus, *G(t)* at time *t*, taking into account both the high frequency – Rouse relaxation of the polymer (for describing the relaxation of molecular segments shorter than the molar mass between two entanglements) and the disentanglement relaxation function $G_d(t)$, which includes a classical description of reptation, contour length fluctuations, and constraint release processes:

$$G(t) = G_d(t) + \sum_i \varphi_i \left(\frac{\rho RT}{M_i} \sum_{p=Z_i+1}^{n} \exp\left(\frac{-p^2 t}{\tau_R(M_i)} \right) + \frac{1}{4} \frac{\rho RT}{M_i} \sum_{p=1}^{Z_i} \exp\left(\frac{-p^2 t}{\tau_R(M_i)} \right) \right) \quad (1)$$

$$G_d(t) = G_N^0 \left(\sum_i \varphi_{linear,i} \int_0^1 p_{rept}(x_{lin}, t) \; p_{fluc}(x_{lin}, t) \; dx_{lin} \right)^{\alpha+1} \quad (2)$$

where G_N^0 is the plateau modulus, $\varphi_{linear,i}$ are the weight fractions of the different linear chains, ρ is the polymer density, T is the temperature and $\tau_R(M_i)$ is the Rouse relaxation time of a chain of mass M_i and proportion φ_i. Furthermore $p_{rept}(x,t)$ and $p_{fluc}(x,t)$ are the survival probabilities of the initial tube segments localized at the normalized position x (going from 0 at the chain extremity to 1, at the middle) at time t, for the reptation and contour length fluctuations processes, respectively. The $(\alpha+1)$ exponent takes into account the dynamic tube dilution process, with the dilution exponent α being fixed to 1.[3-4] By summing up these survival probabilities along all the chains according to their proportion at time *t*, the total unrelaxed fraction of the polymer at this specific time is then obtained.

As explained in details in refs. 5 and 6, the survival probabilities $p_{rept}(x,t)$ and $p_{fluc}(x,t)$ can be described by time-decreasing exponential functions, which depend, respectively, on the reptation and fluctuations times of the different molecular segments along the chains. Finally, from the relaxation function *G(t)*, the storage and loss moduli are determined using the Schwarzl functions.[7]

Material parameters:

The material parameters required in our tube-based model are the plateau modulus, the average molar mass between two entanglements and the Rouse time of an entanglement segment. As detailed in Section IV.2, these parameters have been fixed by best-fitting procedure, based on the rheological response for non-functionalized PEO chains, and consistently with literature values.[8]

1. S. Z. D. Cheng, A. Zhang, J. S. Barley, J. Chen, A. Habenschuss and P. R. Zschack, Macromolecules, 1991, **24**, 3937.

2. S. W. Lee, E. Chen, A. Zhang, Y. Yoon, B. S. Moon, S. Lee, F. W. Harris and S. Z. D. Cheng, Macromolecules, 1996, **29**, 8816.

3. E. van Ruymbeke, Y. Masubuchi and H. Watanabe, Macromolecules, 2012, **45**, 2085.

4. E. van Ruymbeke, V. Shchetnikava, Y. Matsumiya and H. Watanabe, Macromolecules, 2014, http://dx.doi.org/10.1021/ma501566w.

5. E. van Ruymbeke, R. Keunings and C. Bailly, J. Non- Newtonian Fluid Mech., 2005, **128**, 7.

6. E. van Ruymbeke, C. Bailly, R.Keunings, D. Vlassopoulos, Macromolecules, 2006, **39**, 6248.

7. F.R. Schwarzl, Rheol. Acta, 1971, **10**, 166.

For Table of Content Only: